Hydrothermal Synthesis of MnV_2O_6 Nanorods as an Anode Material for Lithium-ion Batteries

Lin Li[1, 2,*], *Wei* Zheng[1], *Rongfei* Zhao[1] and *Jinsong* Cheng[1]

[1]School of Chemistry and Chemical Engineering ,Anshun University, Anshun 561000, China
[2]School of Chemical Engineering, Guizhou University of Engineering Science, Bijie, China

Abstract. The MnV_2O_6 nanorods anode materials was prepared by a simple hydrothermal method, $MnCl_2 \cdot 2H_2O$ and NH_4VO_3 as raw stuffs. The MnV_2O_6 nanorods anode materials were tested by SEM, XRD, and galvanostatic charge/discharge profile measurement. Time-dependent experiments were designed to examine the morphology evolution of the MnV_2O_6 nanorods anode materials. As an anode material, the MnV_2O_6 nanorods showed the good discharge capacity (403 mAh g^{-1} of 100th). The good electrochemical performance can be attributed to the synergistic effect with Mn and V elements, and fast lithium ion diffusion of the 1D nanorods structure.

1 Introduction

Lithium ion battery (LIBs) have been more and more widely used with pure electric vehicles, hybrid electric vehicles, mobile electronic products, et.al [1]. However, commercialization anode material (graphite: 372 mAh g^{-1}) limit the further development and application of LIBs. So the development of low cost, non-toxic, long cycle life of electrode materials become the urgent demand of the LIBs [2]. In all TMOs (transition metal oxides), metal vanadates have be used incatalytic, optical, and electrode materials fields [3]. According to the literature, metal vanadates (such as $Co_3V_2O_8$, CoV_2O_6, $FeVO_4$, MoV_2O_8, $Ni_3V_2O_8$, and $Cu_3V_2O_8$) also have good electrochemical performance, which can be used well in electrode materials (lithium-ion batteries, sodium-ion battery, zinc ion battery, et al.) [4−6].

MnV_2O_6 have generated remarkable attention because of the facile preparation, safety, and high theoretical capacity. Some reports were related to research it as anode materials, the electrochemical property of pure MnV_2O_6 is dissatisfactory, they have modified the MnV_2O_6 by means of coating, compounding and constructing nanostructures to achieve the purpose of improving electrochemical performance. Kim and Ikuta synthesized a brannerite structure MnV_2O_6 by a polymer gelation method, and the MnV_2O_6 electrode material displayed a high initial discharge capacity [7]. In this work, the MnV_2O_6 nanorods anode materials was prepared by a simple hydrothermal method. The morphology, crystal structure and electrochemical properties of the prepared composites were systematically investigated.

* Corresponding author: 404003375@qq.com

Time-dependent experiments were designed to examine the morphology evolution of the MnV_2O_6 nanorods anode materials.

2 Experimental

Firstly, $MnCl_2{\cdot}2H_2O$ and NH_4VO_3 with stoichiometric amounts ratio of 1:2 were dissolved in 30 ml distilled water under magnetic stirring for 1 h. Then the mixed solution was transferred into a 50 mL teflon-lined stainless steel autoclave and annealed at 180 °C for 24 h. After naturally cooled down to room temperature, the resulting product was collected by filtration, and washed with deionized water and absolute alcohol for three times. It was further dried at 60 °C for 12 h.

The crystal structure and surface morphologies of the MnV_2O_6 were characterized by X-ray diffraction (XRD) with Cu Kα radiation (Bruker AXS, D8 diffractometer) and scanning electron microscopy (SEM; JEOL JSM, 6510 V).The typical Electrochemical measurements process of MnV_2O_6 material could be briefly shown in ref [8].

3 Results and discussion

The morphologies of the as-obtained MnV_2O_6 sample was measured via SEM. The morphology of the MnV_2O_6 sample was shown in Fig. 1a and b, which emerges severe aggregation of irregular nanorods structure, and the nanorods morphology of MnV_2O_6 sample is composed of non-uniform nanorods (diameters of ~ 200 nm and length of 2~10 μm). Fig.1c showed the XRD patterns of the MnV_2O_6 nanorods sample. The diffraction peaks can be indexed to the cubic phase of MnV_2O_6 (JCPDS No.35-0139).The identified diffraction peaks at14.2, 20.0, 20.6, 27.2, 28.2, 29.3, 36.8, 38.6, 40.5, 40.7, 41.8, 43.5, 47.3, 47.8, 48.3, 51.7, 54.3, and 55.7º can be well assigned to (001), (20-1), (200), (110), (20-2), (201), (-112), (-311), (310), (111), (202), (003), (311), (-403), (-113), (020), (-204), and (-113) planes of MnV_2O_6. The MnV_2O_6 sample exhibit sharp diffraction peaks, indicating the well crystallization.

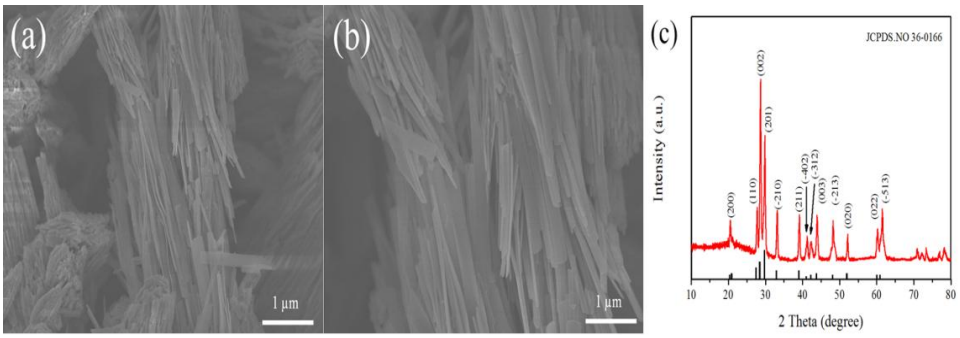

Fig. 1. SEM images (a and b) and XRD pattern (c) of the MnV_2O_6.

To confirm the formation mechanism of the MnV_2O_6 nanorods, time-dependent experiments were designed to examine the morphology evolution of the sample under different reaction times in Fig. 2. The morphologies of the as-obtained five compounds were measured via SEM. The morphology of the MnV_2O_6 (1 h) was shown in Fig. 2a, which emerges severe aggregation of irregular particles. After reaction time of 3 h, the morphology changed significantly, the morphology was made up nanoparticles and nanorods. As the reaction time continued to increase, the morphology continued to change. After reaction time of 12 h, the morphology was consisted of a small number of

nanoparticles and a mass of nanorods. The 1D nanorods structure is beneficial to lithium ion diffusion [9].

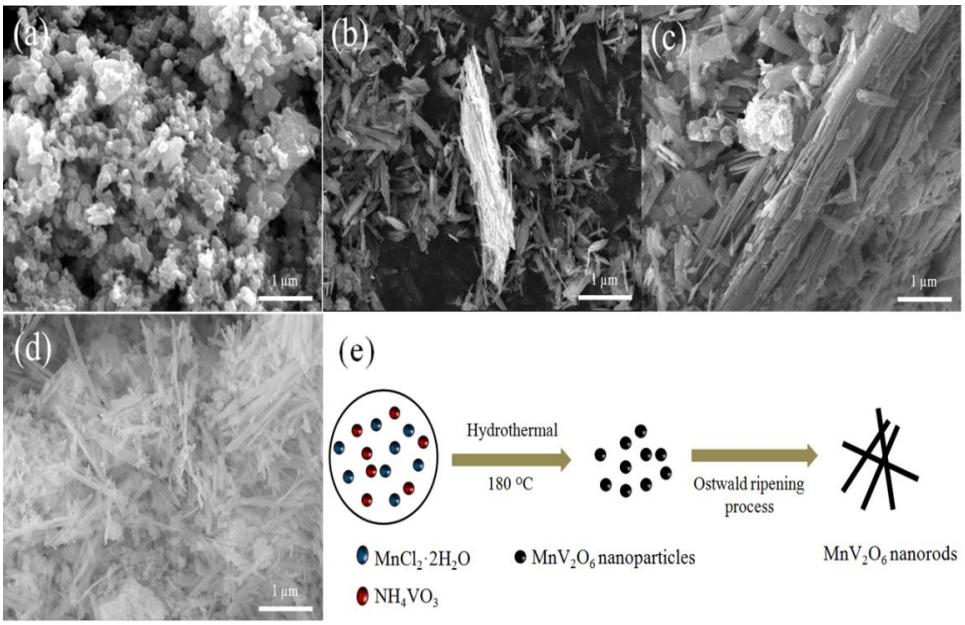

Fig. 2. SEM images of the precursors obtained after different reaction times: (a) 1 h, (b) 6 h, (c) 6 h, and (d) 12 h. (e) Schematic illustration of the formation process for the MnV_2O_6 nanorods.

Fig. 3a shows the discharge-charge curves of the MnV_2O_6 electrode at a constant current density of 200 mA g^{-1}. The beginning discharge specific capacity of the MnV_2O_6 electrode is 1123 mAh g^{-1}, which can be attributed to store 10.2 Li mole of MnV_2O_6. The extra specific capacity can be attributed to the SEI (solid electrolyte interphase) layer, which be formed by the decomposition of solvent in the electrolyte solution [10]. It can be seen that the MnV_2O_6 electrode is 709.6 mAh g^{-1} of the 2nd cycle, which means 36.8% of the first capacity loss. The samples respectively retain capacity of 403 mAh g^{-1} of 100th cycle. Huang and Gao synthesized uniform MnV_2O_6 nanobelts as anode materials by a hydrothermal method; the MnV_2O_6 nanobelts displayed high cycling stability (1085 mAh g^{-1} at 100 mA g^{-1}) and rate capability [11]. Some research work to improve rate performances by coating or composite method for its application in our working. For example, polymer coating of MnV_2O_6 materials and MnV_2O_6/graphene nanocomposites are also well known to be for improving electrode performance because it is simple, low cost, and scalable. The MnV_2O_6 nanorods electrode exhibits higher capacity. Outstanding electrochemical properties for the MnV_2O_6 nanorods attributed to one dimensional nanorod structure can provided a larger surface area, shorter lithium ion diffusion path, maintain stable structure, guaranteed the good rate performance[4]. Fig. 3c shows the CV curves of MnV_2O_6 electrode at 0.1 mV s^{-1}. During the first cathodic scans, the peaks of MnV_2O_6 electrode at 1.89, 1.30, 0.63, 0.41 and 0.05 V were corresponding to the reduction of MnO and V_2O_5 to form Mn^0 and $Li_{x+y}V_2O_5$ as well as formation of SEI. In the following scan, the reduction peaks moved to 0.74 V and 0.50 V. The anodic scans feature three oxidation peak at 0.19, 0.65, 0.85 and 2.52V, which could be associated with the oxidations of Mn to MnO, $Li_{x+y}V_2O_5$ to $Li_xV_2O_5$ and the decomposition of Li_2O. Furthermore, the CVs of MnV_2O_6 electrode remain almost the same of the follow cycle, which can also indicate that the good

rate performance of MnV_2O_6 electrode. The possible electrochemical reactions of the MnV_2O_6 electrode was as follows [7,11]:

$$MnV_2O_6 + x\ Li^+ + xe^- \rightarrow MnO + Li_xV_2O_5 \quad (1)$$

$$MnO + 2Li+ + 2e- \rightarrow Mn + Li2O \quad (2)$$

$$LixV2O5 + yLi+ + ye- \rightarrow Lix+yV2O5 \quad (3)$$

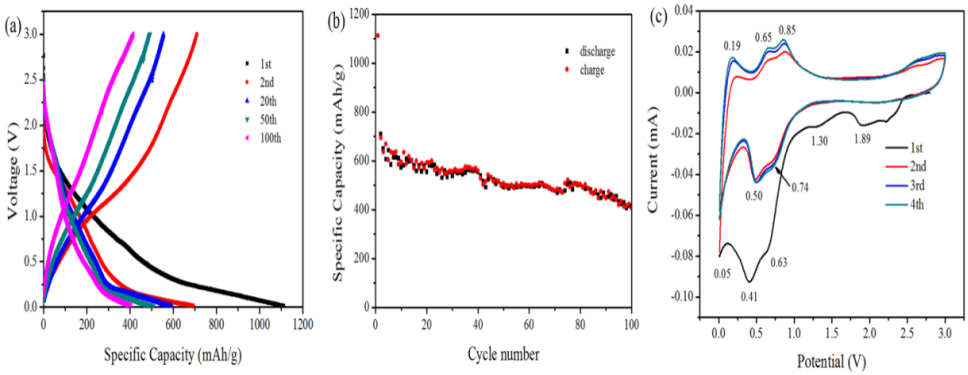

Fig. 3. (a) Discharge-charge curves of the MnV_2O_6 sample for the 1st, 2nd, 20th, 50th and 100th cycles at a constant current density of 200 mA g^{-1}, (c) Cycling performance of the MnV_2O_6 electrode, (c) cyclic voltammograms of the MnV_2O_6 electrode at the rate of 0.1 mV s^{-1}.

4 Conclusions

In this work, the MnV_2O_6 nanorods anode materials was prepared by a simple hydrothermal method, $MnCl_2{\cdot}2H_2O$ and NH_4VO_3 as raw stuffs. The MnV_2O_6 nanorods anode materials were tested by SEM, XRD, and galvanostatic charge/discharge profile measurement. Time-dependent experiments were designed to examine the morphology evolution of the MnV_2O_6 nanorods anode materials. As an anode material, the MnV_2O_6 nanorods showed the good discharge capacity (403 mAh g^{-1} of 100th). The good electrochemical performance can be attributed to the synergistic effect with Mn and V elements, and one dimensional nanorod structure can provided a larger surface area, shorter lithium ion diffusion path, and maintain stable structure.

5 Acknowledgments

This work was financially supported by the joint science and technology funds of the Guizhou Provincial Education Department (No. KY [2018] 031).

References

[1] H. Baea, Y. Kim, Mater. Adv. **2**, 3234 (2021)

[2] H. Zheng, Q. Zhang, H. Gao, W. Sun, H.M. Zhao, C.Q. Feng, J.F. Mao, Z.P. Guo, Energy Storage Mater. **22**, 128 (2019)

[3] M. Inagaki, T. Morishita, M. Hirano, V. Gupta, and T. Nakajima, Solid State Ionics **156**, 275 (2003)

[4] Y. Liu, Y.G. Zhang, J. Du, W.C. Yu, Y.T. Qian, J. Crystal Growth **291**, 320 (2006)

[5] K. Hua, X. J. Li, Z.W. Fu, D. Fang, R.Bao, J.H. Yi, Z.P. Luo, J. Solid State Chem.**237**,287 (2019)

[6] S.S. Kim, H. Ikuta, M. Wakihara, Solid State Ionics **139**, 57 (2001)

[7] S.J. Lei, K.B. Tang, Y Jin, C.H. Chen, Nanotechnology **18**, 175605 (2007)

[8] Y.C. Ji, J. Hu, J.Biskupek, U. Kaiser, Y.F. Song, C. Streb, Chem. Eur. J. **23**, 16637 (2017)

[9] S.Y. Zhang, Y.Y. Zhang, RSC Adv. **5**, 91441 (2015)

[10] X.L. Liu, Y.C. Cao, H. Zheng, X. Chen, C.Q. Feng, Appl. Surf. Sci. **394**, 183 (2017)

[11] W.D. Huang, S.K. Gao, X.K. Ding, L.L. Jiang, M.D. Wei, J. Alloy. Compd. **495**, 185 (2010)